High Specific Surface Area in Nanometric Carbonated Hydroxyapatite

S. Padilla,[†] I. Izquierdo-Barba,[†,‡] and M. Vallet-Regí*[,†,‡]

Departamento Química Inorgánica y Bioinorgánica, Facultad de Farmacia, and Centro de Investigación Biomédica en Red. Bioingeniería, Biomateriales y Nanomedicina, Spain

Received June 15, 2008
Revised Manuscript Received August 1, 2008

Nowadays, one of the challenges of the scientific community of biomaterials is to obtain carbonated apatites, nonstoichiometric, with nanometric size, equivalent to biological ones as raw material for the manufacture of ceramic implants and 3D macroporous scaffolds for tissue engineering. The synthesis of apatites with nanometric size is not very difficult; in fact, a high number of works about that have already been published.[1−3] However, an apatite with all characteristics of the biological apatites in the same material (that is, nonstoichiometric, with particle size lower than 50 nm, containing carbonate (4−8%), HPO_4^{2-} and labile ions with a high specific surface area) is a challenge that has not been achieved yet. In addition, for the preparation of implants and scaffolds is necessary to have high amounts of sample. For that, it is necessary to use a simple method of synthesis, which allows to obtain massive and reproducible amounts of such material. Herein, the possibility to obtain large amounts of a synthetic apatite similar to biological ones, not only in composition but also in particle size, stoichiometry, crystallinity, and specific surface area, is described.

The mineral phase of the bone is a nanocrystalline hydroxyapatite with about 4−8% of carbonate and other ionic substitutions like HPO_4^{2-}, Na^+, Mg^{2+} or trace ions such as F^-, Cl^-, K^+, and Sr^{2+}.[4−6] The crystals are platelet-like (elongated along the crystallographic *c*-axis), extremely small, about 50 nm by 25 nm by 4 nm thickness.[6−8] The apatite in the bone tissue is characterized by its low stability and high reactivity. These features are related with its small dimensions, low crystallinity, high specific surface area, its nonstoichiometric composition, presence of other ions in the crystal lattice, inner crystalline disorder, and labile ions at the crystal surface.[4−8]

Several techniques have been used for hydroxyapatite preparation.[3,5,6,9] These methods can be classified in two groups, solid-state reactions and wet methods. The latest includes precipitation, hydrothermal, hydrolysis of other calcium phosphates, calcium phosphate cements, and biomimetic methods. In spite of the variety of methods reported, the obtention of an apatite similar to the biological ones is nowadays very complicated, even more if a massive amount is necessary. Some deficiencies of the synthetic apatite are the lower CO_3^{2-} content, the larger particle size and the smaller specific surface area compared to the biological ones.[9] In addition, the apatite obtained by some methods, such as the biomimetic ones, is only available in small amounts. It is also worth noting that, although several calcium phosphate biomaterials are clinically used at the moment, most of them are highly crystalline materials, with very slow reabsorption and reactivity and therefore with a different behavior to that of biological apatites.[10,11]

In this work, we report the synthesis of a nanocrystalline carbonated hydroxyapatite (CHA) with similar characteristics to the bone apatite using a simple precipitation method. The synthesis was carried out in a crystallization equipment described elsewhere.[12] Two solutions were prepared: (solution A) 1 L of 1 M $Ca(NO_3)_2 4H_2O$ (Aldrich) and (solution B) 1 L of 0.6 M $(NH_4)_2HPO_4$ (Merck) and 0.3 M $(NH_4)_2CO_3$ (Riedel-de Häen). The pH of this solution was adjusted to 9.2 by adding a NH_4OH solution (Riedel-de Häen). Both solutions were dropped simultaneously into the reactor at a flow rate of 30 mL/min. The temperature was maintained at 37 °C during the synthesis. At the beginning, the stirring speed was adjusted to 200 rpm and it was gradually increased during the solution addition to 800 rpm. After the solution addition, the resulting suspension was stirred for 10 min at 2400 rpm. Afterward, the suspension was quickly vacuum-filtered. The resulting cake was washed with abundant lukewarm water. After that, the cake was freezed at −80 °C for 4 h. Finally, it was freeze-dried for 24 h at a freezing speed of 54 g/h.

The content of Ca and P in the CHA was determined by X-ray fluorescence and the carbon content obtained by elemental analysis. The specific surface area was determined by N_2 adsorption using the BET method. The sample was also characterized by X-ray diffraction (XRD), by Fourier transform infrared spectroscopy (FTIR), and transmission electron microscope (TEM).

The sample obtained has a Ca/P rate of 1.71 ± 0.04 and a content of CO_3^{2-} equal to 8.0 ± 0.3%, which is in the range of the bone apatite. By XRD (Figure 1) a characteristic pattern of nanocrystalline apatite is observed.

* To whom correspondence should be addressed. E-mail: vallet@farm.ucm.es.
† Universidad Complutense de Madrid.
‡ CIBER-BBN.

(1) Driessens, F. C. M.; Boltong, M. G.; de Maeyer, E. A. P.; Wenz, R.; Nies, B.; Planell, J. A. *Biomaterials* **2002**, *23* (19), 4011–4017.
(2) Welzel, T.; Meyer-Zaika, W.; Epple, M. *Chem. Commun.* **2004**, (10), 1204–1205.
(3) Vallet-Regi, M.; Arcos Navarrete, D. *Biomimetic Nanoceramics in Clinical Use. From Materials to Applications*; Society of Chemistry: London, 2008.
(4) LeGeros, R. Z. *Calcium Phosphates in Oral Biology and Medicine*; Myers, H. M. Ed.; Karger: London, 1991; Vol. 15.
(5) Elliot, J. C. *Structure and Chemistry of the Apatites and Other Calcium Orthophosphates*. Elsevier: Amsterdam, 1994; Vol. 18.
(6) Vallet-Regi, M.; Gonzalez-Calbet, J. M. *Prog. Solid. State Chem.* **2004**, *32*, 1.
(7) Lowenstam, H. A.; Weiner, S. *On Biomineralization*. Oxford University Press: New York, 1989.
(8) Weiner, S.; Wagner, H. D. *Annu. Rev. Mater. Sci.* **1998**, *28*, 271.
(9) Vallet-Regi, M. *Dalton Trans.* **2001**, 97.
(10) Tadic, D.; Epple, M. *Biomaterials* **2004**, *25*, 987.
(11) LeGeros, R. Z. *Clin. Orthop. Relat. Res.* **2002**, *395*, 81.
(12) Rodriguez-Lorenzo, L. M.; Vallet-Regi, M. *Chem. Mater.* **2000**, *12*, 2460.

10.1021/cm801626k CCC: $40.75
Published on Web 09/11/2008

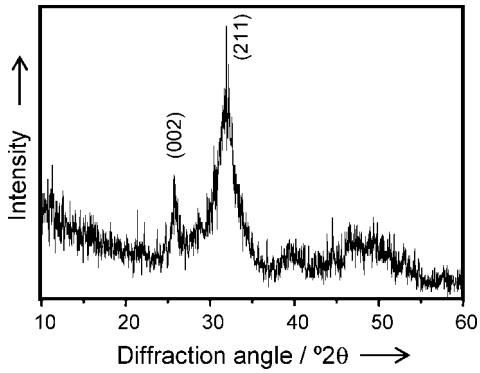

Figure 1. XRD pattern of the obtained CHA corresponding to a nanocrystalline apatite.

The FTIR spectrum (Figure 2a) shows bands corresponding to PO_4^{3-} (ν_3-1034, ν_1-960, ν_4-604, ν_4-565 cm^{-1}) and CO_3^{2-} (ν_3-1474, ν_3-1419, ν_2-873 cm^{-1}). To get more information about the composition and structure of the sample, the FTIR was deconvoluted in the ν_2 CO_3^{2-} and ν_4 PO_4^{3-} domains. The deconvoluted FTIR spectrum in the ν_2 CO_3^{2-} domains (Figure 2b) exhibits three bands at 879, 873, and 866 cm^{-1}, which are similar to the characteristic ones observed in bone crystals.[13,14] These bands mean that the carbonate ions are present in the CHA structure, in the two possible position, that is: carbonate ions substituting the hydroxyl ions (type A carbonated apatite, 879 cm^{-1}) and carbonate ions substituting the phosphate ions (type B carbonated apatite, 873 cm^{-1}), being the latest the majoritary substitution. In addition, labile carbonate ions are also present (866 cm^{-1}).[14] In the ν_4 PO_4^{3-} domain (Figure 2c) the most intense bands located at 604, 575, and 563 cm^{-1} are assigned to PO_4^{3-} ions in apatite sites. HPO_4^{2-} in apatite environment is also observed at 547 cm^{-1}. In addition, phosphate (614 cm^{-1}) and HPO_4^{2-} (533 cm^{-1}) bands in nonapatite environment are observed. The FTIR results show that the obtained sample is an AB-type carbonated apatite where the most of CO_3^{2-} are substituting the phosphate ions. This sample also contains HPO_4^{2-} ions in the apatitic structure. In addition, labile ions (PO_4^{3-}, CO_3^{2-} and HPO_4^{2-}) in nonapatite sites are present. This behavior is similar to that observed in biological apatites.

In images a and b in Figure 3, TEM microgrographs show the very small size of CHA nanoparticles having needle shape morphology, mostly agglomerated. The particle has a length of 15−20 nm and width of 3−5 nm (images a and b in Figure 3). Fourier diffractogram, taken from high-resolution transmission electron microscopy (HRTEM) image, shows diffused rings characteristic of a nanocrystalline sample. HRTEM image evidence that needle shaped particles show *d*-spaces of 0.34 and 0.28 nm corresponding to the 002 and 211 reflection of an apatitelike phase as observed by XRD.

The high specific surface area (SSA) of the obtained sample is a very interesting result since it is as high as 300

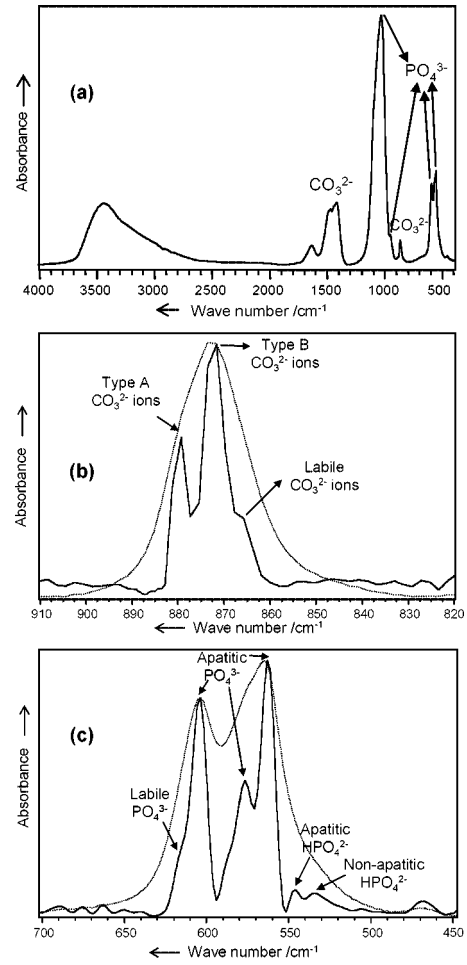

Figure 2. (a) FTIR spectrum of CHA showing the bands characteristic of a nanocrystalline carbonated hydroxyapatite. (b) --- Nondeconvoluted and — deconvoluted FTIR spectrum of CHA in the ν_2 CO_3^{2-} domains (bandwidth 14 cm^{-1}; sensitivity coefficient 2.7). The two types of possible substitution of CO_3^{2-} are observed (type A, CO_3^{2-} substituting the OH^- groups; and type B, CO_3^{2-} substituting the PO_4^{3-} groups). In addition, a labile nonapatite CO_3^{2-} environment can be observed. (c) --- Nondeconvoluted and — deconvoluted FTIR spectrum of CHA in the ν_4 PO_4^{3-} domains (bandwidth 22 cm^{-1}; sensitivity coefficient 2.3). PO_4^{3-} and HPO_4^{2-} in apatite environment are observed. In addition these ions in nonapatitic sites are present.

± 10 m^2/g. The isotherm of the CHA (see the Supporting Information, Figure SI1a) corresponds to a type IV isotherm, according to the IUPAC classification, showing a hysteresis loop at $P/P^0 > 0.4$. The pore volume is 0.46 cm^3/g. The sample shows (see the Supporting Information, Figure SI1b) a wide pore distribution of micropores centered at 0.48 nm and mesopores centered at 4.2 nm. The wide distribution of mesopores corresponds to the space between nanoparticles which are agglomerated, as observed in TEM images.

To the best of our knowledge, there is no report about apatites, obtained by a similar method, showing so high specific surface area. It is worth noting that the specific surface area of most hydroxypatite reported, even previous to calcination, is lower than 100 m^2/g.[12,15,16] This high value of surface area is related to the small size of the particles.

(13) Kim, H. M.; Rey, C.; Glimcher, M. J. *J. Bone Miner. Res.* **1995**, *10*, 1589.
(14) Rey, C.; Collins, B.; Goehl, T.; Dickson, I. R.; Glimcher, M. J. *Calcif. Tiss. Int.* **1989**, *45*, 157.
(15) Koutsopoulos, S. *J. Biomed. Mater. Res.* **2002**, *62*, 600.
(16) Jokanovic, V.; Izvonar, D.; Dramicanin, M. D.; Jokanovic, B.; Zivojinovic, V.; Markovic, D.; Dacic, B. *J. Mater. Sci.: Mater. Med.* **2006**, *17*, 539.

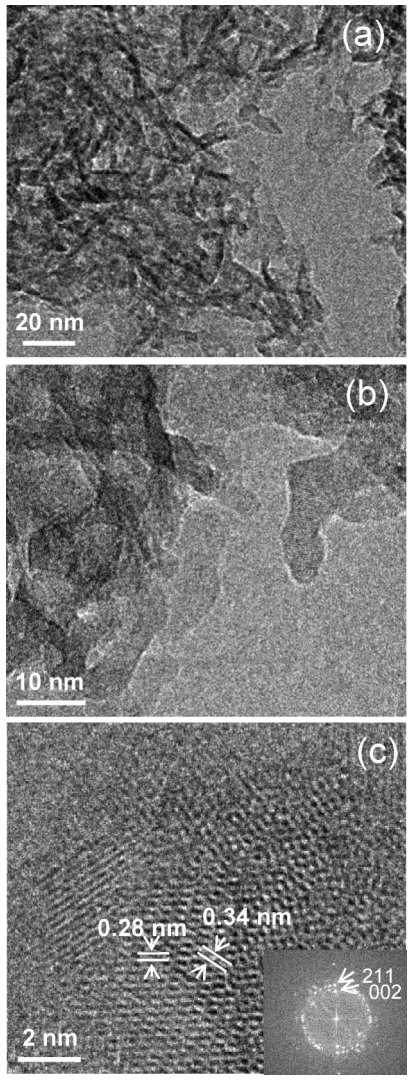

Figure 3. TEM images of CHA taken at different magnification (60 000, 300 000 and 600 000 K, respectively). (a, b) Low-magnification images show the small size and the needle-like shape of the nanoparticles. (c) HRTEM image and its corresponding Fourier diffractogram show the *d*-spacing corresponding to the 002 and 211 reflections of an apatite phase.

In addition, it had been documented that ionic substitutions in hydroxyapatite, like carbonate ions, increase the surface area. The dried and calcination treatments of CHA are very important for the SSA. For example, drying the CHA at 100 °C for 24 h instead of freeze-dried reduced the SSA in ca. 100 m^2/g and the heat treatment at 900 °C for 1 h reduced the SSA to 10 m^2/g.

The obtained CHA shows characteristics that are very important for the biological behavior. For example, as mentioned above, the bone apatite crystals have a high specific surface area, being one of the key factors for the high reactivity and solubility of this mineral. The CO_3^{2-} incorporation in the PO_4^{3-} group position (type B carbonated apatite) is the majoritary in biological apatites as well as in this sample and it has been shown to cause a decrease in the crystallinity and an increase in the hydroxyapatite solubility.[4−6] The presence of labile CO_3^{2-}, PO_4^{3-}, and HPO_4^{2-} ions is considered of great importance for the properties of nanocrystals, specially concerning maturation, ionic exchange, and adsorption.[17] According to the proposed model by Rey et al.[17] for nanocrystalline apatite, crystals of the obtained sample should be formed by a core of apatite lattice and a hydrated layer containing relative mobile ionic species (nonapatite environments) at the crystals surface.

Summarizing, a reproducible method for the synthesis of CHA equivalent to bone apatite is proposed. Nanocrystalline and nanometric (15−20 nm by 3−5 nm) carbonated hydroxyapatite with a very high specific surface area (300 m^2/g), a high content of carbonate (8%, in the range of the bone apatite), with HPO_4^{2-} and labile ions like PO_4^{3-}, CO_3^{2-} and HPO_4^{2-}, has been obtained. A precipitation method and the fallowing conditions were employed in the synthesis: low synthesis temperature (37 °C), short time of precipitation (35 min) and aging (10 min), and freeze-drying. With this method, it is possible to obtain more than 100 g of sample in 45 min, allowing us to have a homogeneous material, with similar characteristics to the biological apatite. It is important to highlight the high specific surface area of the obtained material. That not only means a high reactivity, but also the possibility of adsorbing many active agents, like proteins, growth factor, DNA, etc.

The possibility to obtain nanoapatites with similar characteristics to the biological ones in large amounts will allow us to use these nanoparticles in future works in the obtention of 3D macroporous scaffolds for tissue engineering.

Acknowledgment. Financial support by the Spanish CICYT (Mat2005-01486) and CAM P-Mat-000324-0505 is gratefully acknowledged.

Supporting Information Available: N_2 adsorption−desorption isotherm and pore size distribution of CHA (PDF). This material is available free of charge via the Internet at http://pubs.acs.org.

CM801626K

(17) Cazalbou, S.; Combes, C.; Eichert, D.; Rey, C. *J. Mater. Chem.* **2004**, *14*, 2148.